1481

Practical considerations of DW-MRS with ultra-strong diffusion gradients

Christopher Jenkins[1], Elena Kleban[1], Lars Mueller[1], John Evans[1], Umesh Rudrapatna[1], Derek Jones[1], Francesca Branzoli[2], Itamar Ronen[3], and Chantal M.W Tax[1]
[1]CUBRIC, School of Psychology, Cardiff University, Cardiff, United Kingdom, [2]Centre for NeuroImaging Research - CENIR, Brain and Spine Institute - ICM, Paris, France, [3]Department of Radiology, Leiden University Medical Center, Leiden, Netherlands

Synopsis

Diffusion-weighted magnetic resonance spectroscopy benefits from the use of ultra-strong gradients. Slow diffusing metabolites necessitate a large range of b-values to accurately model the diffusion properties. Ultra-strong gradients open the possibility of higher b-values and reduced diffusion times, alleviating some of these constraints. We present initial data acquired with DW-PRESS on a 300mT/m gradient Connectom scanner, and introduce the practical considerations associated with ultra-strong gradients.

Introduction

The ubiquity of water molecules, and their presence both within cells, and in the extracellular space, complicates the interpretation of diffusion-weighted imaging data. Diffusion-weighted magnetic resonance spectroscopy (DWMRS) utilises MRS as a filter, sensitising the MR signal to different metabolites, which are almost exclusively intra-cellular, with some considered predominantly glial – Myo-inositol (Ins) and choline compounds (TCho) – and others predominantly neuronal – N-acetyl-aspartate (NAA) and glutamate [1].

The apparent diffusion coefficients (ADC) of metabolites are typically smaller than those of water [2], which necessitates a larger range of b-values to characterise metabolite diffusion properties. DW-STEAM can reach high b-values by facilitating long diffusion times independent of T_2 relaxation, providing an attractive approach. DW-PRESS offers improved SNR, however diffusion times are coupled to T_2, reducing its effective b-value range. Ultra-strong gradients remedy this, providing access to larger b-values for a given T_E (Fig.1). Ultra-strong gradients also allow shorter diffusion times, while maintaining the required b-value range. This can reduce the variability resulting from pulsation, and can provide additional cell-specific microstructural properties [3, 4].

In this work, we present initial data acquired using a DW-PRESS sequence, and practical considerations of introducing ultra-strong gradients. Specifically, SNR will be low at very high b-values, and eddy currents become increasingly prevalent at larger gradients amplitudes, an issue which is further compounded by the low SNR of water for high b-values. This necessitates efficient pre-processing of MRS data, to maximise the available SNR. Finally, gradient non-linearities modulate the b-matrix and voxel geometry, this must be corrected in order to obtain reliable estimates [5].

Materials and methods

Two healthy subjects were recruited for this study, and scans were conducted using a 3T Connectom research only scanner equipped with 300mT/m gradient coil and a modified 32-channel head coil (Siemens Healthcare, Erlangen, Germany). DW-PRESS data were acquired with T_R=2500ms, T_E=70ms, bandwidth=4000Hz, and 2048 complex points. Diffusion weighting was applied along three orthogonal axes using single gradients, with 7 b-values in each case, plus an acquisition at b=0. The diffusion time, $\Delta \sim T_E/2$=35ms, and nominal b-values were: 0, 620, 1395, 2480, 5579, 9918, 15497, and 21578 s/mm^2. 24 water-suppressed, and 8 water-unsuppressed averages were acquired with cardiac triggering. Voxel positioning and diffusion directions can be found in Fig.2.

Weighted coil combination and phasing was performed using the water-unsuppressed b0 acquisition [6]. To reduce the effects of motion, corrupted averages were identified using a likeliness metric, and omitted prior to spectral registration [7]. Eddy current correction was performed using unsuppressed water, with the phase extracted via LPSVD [8]. Tarquin [9] was used for spectral fitting, incorporating macromolecular and lipid models into a fitting basis set, with the baseline approximated by a Gaussian window function.

Results & discussion

Representative spectra following pre-processing are shown in Fig.3. Eddy current correction was found to be robust for the b-value range acquired, but the SNR of water would eventually restrict this approach, highlighting a need for alternative methods. Metabolite signals were extracted for each diffusion condition for TNAA(NAA+NAAG), TCr(Cr+PCr), and TCho(PCho+GPC). The b-matrix was corrected for gradient non-linearities using the spatially varying gradient coil tensor provided by the vendor. Effective b-values were obtained by averaging the deviations within a mask localising the voxel (Fig.4). The effect of gradient non-linearity varies with voxel position/dimension and applied diffusion gradient. In our data we observed b-value changes up to 4% of the nominal value. Which, if not corrected, will result in incorrect diffusivity estimates in the ultra-strong gradient regime.

A mono-exponential model was used to fit the b-value dependence of the metabolite amplitudes for the first 5 points, and diffusion coefficients extracted (Fig.5). Fit accuracy inevitably decreases with SNR, so consideration of the Cramer-Rao lower bound was important for maintaining data quality. Metabolite diffusivities, D, along a given axis reflect a mixture of fibre orientations within the voxel. Voxels dominated by fibres parallel or orthogonal to the diffusion gradient result in high or low diffusivities, respectively. Ronen et al [10] found NAA diffusivity values of 0.076 and 0.34 μ m^2 /ms for diffusion gradients orthogonal and parallel to the main fibre orientation, respectively. The voxels considered in this study contain mixed fibre orientations, and obtained TNAA diffusivities between 0.12 and 0.16 μ m^2 /ms are consistent with the findings of other DW-MRS studies [11, 12, 13, 14].

Conclusion

DWMRS with ultra-strong gradients yields improved SNR for large b-values, and allows shorter diffusion times. Our results are in line with literature values, and pave the way to study the diffusion of metabolites in previously inaccessible regimes.

Acknowledgements

We are grateful to Fabrizio Fasano from Siemens Healthcare GmbH for his support.

CMWT is supported by a Rubicon grant (680-50-1527) from the Netherlands Organisation for Scientific Research (NWO) and a Sir Henry Wellcome Fellowship (215944/Z/19/Z).

CJ, LM, and DKJ are supported by a Wellcome Trust Strategic Award (104943/Z/14/Z), and DKJ by a Wellcome Trust Investigator Award (096646/Z/11/Z).

References

[1] Choi, J. K., Dedeoglu, A., & Jenkins, B. G. (2007). Application of MRS to mouse models of neurodegenerative illness. NMR in Biomedicine: An International Journal Devoted to the Development and Application of Magnetic Resonance In vivo, 20(3), 216-237.

[2] Ellegood, J., Hanstock, C. C., & Beaulieu, C. (2011). Considerations for measuring the fractional anisotropy of metabolites with diffusion tensor spectroscopy. NMR in Biomedicine, 24(3), 270-280.

[3] Jones, D. K., Alexander, D. C., Bowtell, R., Cercignani, M., Dell'Acqua, F., McHugh, D. J., ... & Tax, C. M. (2018). Microstructural imaging of the human brain with a 'super-scanner': 10 key advantages of ultra-strong gradients for diffusion MRI. NeuroImage, 182, 8-38.

[4] Setsompop, K., Kimmlingen, R., Eberlein, E., Witzel, T., Cohen-Adad, J., McNab, J. A., ... & Cauley, S. F. (2013). Pushing the limits of in vivo diffusion MRI for the Human Connectome Project. Neuroimage, 80, 220-233.

[5]Bammer, R., Markl, M., Barnett, A., Acar, B., Alley, M. T., Pelc, N. J., ... & Moseley, M. E. (2003). Analysis and generalized correction of the effect of spatial gradient field distortions in diffusion-weighted imaging. Magnetic Resonance in Medicine: An Official Journal of the International Society for Magnetic Resonance in Medicine, 50(3), 560-569.

[6] Hall, E. L., Stephenson, M. C., Price, D., & Morris, P. G. (2014). Methodology for improved detection of low concentration metabolites in MRS: optimised combination of signals from multi-element coil arrays. Neuroimage, 86, 35-42.

[7] Near, J., Edden, R., Evans, C. J., Paquin, R., Harris, A., & Jezzard, P. (2015). Frequency and phase drift correction of magnetic resonance spectroscopy data by spectral registration in the time domain. Magnetic Resonance in Medicine, 73(1), 44-50.

[8] Vanhamme, L., Fierro, R. D., Van Huffel, S., & de Beer, R. (1998). Fast removal of residual water in proton spectra. Journal of Magnetic Resonance, 132(2), 197-203.

[9] Wilson, M., Reynolds, G., Kauppinen, R. A., Arvanitis, T. N., & Peet, A. C. (2011). A constrained least-squares approach to the automated quantitation of in vivo 1H magnetic resonance spectroscopy data. Magnetic resonance in medicine, 65(1), 1-12.

[10] Ronen, I., Budde, M., Ercan, E., Annese, J., Techawiboonwong, A., & Webb, A. (2014). Microstructural organization of axons in the human corpus callosum quantified by diffusion-weighted magnetic resonance spectroscopy of N-acetylaspartate and post-mortem histology. Brain Structure and Function, 219(5), 1773-1785.

[11] Kan, H. E., Techawiboonwong, A., Van Osch, M. J., Versluis, M. J., Deelchand, D. K., Henry, P. G., ... & Ronen, I. (2012). Differences in apparent diffusion coefficients of brain metabolites between grey and white matter in the human brain measured at 7 T. Magnetic resonance in medicine, 67(5), 1203-1209.

[12] Najac, C., Branzoli, F., Ronen, I., & Valette, J. (2016). Brain intracellular metabolites are freely diffusing along cell fibers in grey and white matter, as measured by diffusion-weighted MR spectroscopy in the human brain at 7 T. Brain Structure and Function, 221(3), 1245-1254.

[13] Cao, P., & Wu, E. X. (2017). In vivo diffusion MRS investigation of non-water molecules in biological tissues. NMR in Biomedicine, 30(3), e3481.

[14] Ronen, I., Ercan, E., & Webb, A. (2013). Axonal and glial microstructural information obtained with diffusion-weighted magnetic resonance spectroscopy at 7T. Frontiers in integrative neuroscience, 7, 13.

[15] Ganji, S. K., Banerjee, A., Patel, A. M., Zhao, Y. D., Dimitrov, I. E., Browning, J. D., ... & Choi, C. (2012). T2 measurement of J-coupled metabolites in the human brain at 3T. NMR in biomedicine, 25(4), 523-529.

[16] Ke, Y., Cohen, B. M., Lowen, S., Hirashima, F., Nassar, L., & Renshaw, P. F. (2002). Biexponential transverse relaxation (T2) of the proton MRS creatine resonance in human brain. Magnetic Resonance in Medicine: An Official Journal of the International Society for Magnetic Resonance in Medicine, 47(2), 232-238.

Figures

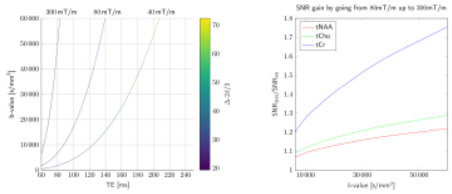

Fig.1. This figure highlights the potential of ultra-strong gradients for DW-MRS. The left panel shows the maximum achievable b-value for DW-PRESS as a function of the echo time for three gradient strengths; 40, 80, and 300 mT/m. The right panel shows the SNR gains resulting from reduced echo time, as a function of b-value. SNR gains calculated using estimates for metabolite T_2 [15, 16].

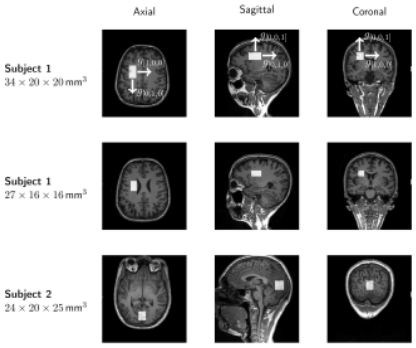

Fig.2. Voxel positioning for the three acquired data sets. Two voxels, predominantly placed in white matter, were acquired, as well as one in the occipital lobe.

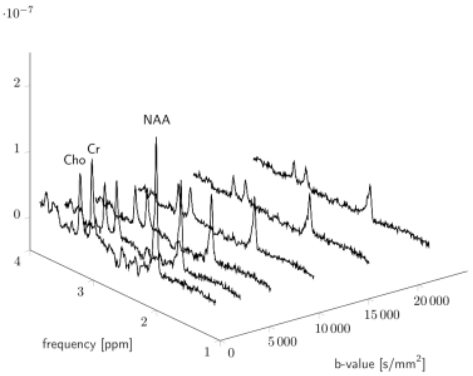

Fig.3. Representative spectra as a function of b-value, following pre-processing. Main features of N-acetyl-aspartate (NAA), creatine (Cr) and choline (Cho) are labelled, for illustration.

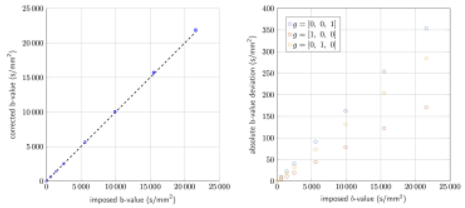

Fig.4. Corrections applied to b-values as a result of gradient non-linearities. The left panel shows the corrected b-values plotted against the corresponding nominal values. The right panel shows the absolute difference as a function of nominal b-value. Colours indicate the directional dependence of the b-value correction.

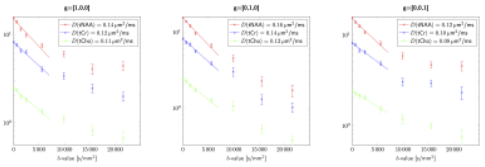

Fig.5. An example of fitting results achieved using a mono-exponential model for the initial 5 points of a single data set. Error bars indicate fit error of metabolites, represented by Cramer-Rao lower bounds.

2714